2014 International Joint Conference on Neural Networks (IJCNN)
July 6-11, 2014, Beijing, China

Completed Hybrid Local Binary Pattern for Texture Classification

Jing-Hua Yuan, De-Shuang Huang*
Computer Science and Technology Department, College of Electronics and Information Engineering
Tongji University
Shanghai, China
yuanjinghua_acer@163.com, dshuang@tongji.edu.cn

Hao-Dong Zhu, Yong Gan
School of Computer and Communication Engineering
Zhengzhou University of Light Industry
Zhengzhou, China
zhuhaodong80@163.com, ganyong@zzuli.edu.cn

Abstract*—The Local Binary Pattern (LBP) and its variants have been widely investigated in image processing and computer vision applications, e.g., texture classification due to their powerful ability to capture image features and computational simplicity. However, owing to the simple selection strategy of the threshold, the original LBP descriptor is sensitive to noise and illumination variations and tends to characterize different local patterns with the same binary code. Recently, the Completed Robust Local Binary Pattern (CRLBP) has been introduced to overcome these demerits, in which the Weighted Local Gray Level (WLG) is introduced to replace the traditional gray value of the center pixel, but the improvement is not significant and one additional parameter has to be tuned. To address these difficulties effectively, this paper proposes a hybrid framework of LBP, called Completed Hybrid Local Binary Pattern (CHLBP), in which a first order derivative and a second order derivative are combined to represent local patterns. In order to make CHLBP more robust and stable, more relationship information among pixels in the local region is exploited, that is, the Average Local Gray Level (ALG) is adopted to take place of the traditional gray value of the center pixel as well as the neighbor pixels. The results obtained from two representative texture databases show that the proposed method is robust to illuminant variations and viewpoint variations and can achieve impressive classification accuracy. The proposed model improves the classification results from 96.95% to 98.78% on the Outex database, and from 91.85% to 94.56% on the UIUC database as compared with the Completed Local Binary Pattern (CLBP), which is the benchmark method of LBP-based models.

Keywords*—*Local Binary Pattern (LBP); Completed Local Binary Pattern (CLBP); Order-based Center-Symmetric Local Binary Pattern (OCS-LBP); Hybrid Local Binary Pattern (HLBP); Completed Hybrid Local Binary Pattern (CHLBP)

I. INTRODUCTION

Texture classification is an active research topic in pattern recognition and computer vision and has been used in many applications, such as biomedical image analysis [26], face recognition [22], and image recognition and retrieval [21]. Generally, texture images captured in the real-world may have obvious orientation variations. Therefore, Rotation invariant texture analysis is immensely needed from both the theoretical and practical viewpoint.

In recent years, numerous approaches for texture feature extraction have been proposed to extract texture features that are rotation and illumination invariant and robust to noise [1]. Davis [2] introduced polarograms and generalized co-occurrence matrices to obtain rotation invariant statistical features. Duvernoy [3] exploited Fourier descriptors to extract the rotation invariant texture feature on the spectrum domain. Goyal *et al*. [4] presented a method based on texel property histogram. Eichmann and Kasparis [5] developed topologically invariant texture descriptors by using line structures extracted by Hough transform. Kashyap and Khotanzad [6] addressed rotation invariant by proposing a circular simultaneous autoregressive (CSAR) model. Cohen *et al*. [7] described texture as Gaussian Markov random fields and estimated rotation angles by using the maximum likelihood estimation. Chen and Kundu [8] exploited multichannel sub-bands decomposition and Hidden Markov Model (HMM) to address rotation invariant. Porter and Canagarajah [9] applied the wavelet transform to texture classification by using the Daubechies four-tap wavelet filter coefficients.

These aforementioned methods have been proven to be rotation invariant, however, they are not very robust to illumination variations. In [10], Ojala *et al*. proposed the Local Binary Pattern (LBP) to address rotation invariant texture classification. As shown in Fig. 2, LBP code is computed by comparing a pixel with its neighbors. A histogram will be built to represent the texture image after the LBP code of each pixel in the image is defined. LBP is a simple yet efficient operator to represent local texture and invariant to monotonic gray scale transformations.

Since Ojala's work, lots of variants of LBP have been proposed. Instead of comparing neighbors with the center pixel, Heikkila *et al*. [11] presented Center-Symmetric LBP (CS-LBP) by comparing center-symmetric pairs of pixels. Liao *et al*. [12] proposed Dominant LBP (DLBP) for texture classification. Tan and Triggs [13] presented Local Ternary Pattern (LTP), extending the conventional LBP to 3-valued codes. However, LTP is no longer strictly invariant to gray-level transformations due to the simple strategy on the

*Corresponding author.

selection of the threshold. Motivated by the order derivative of the LBP, Zhang *et al*. [14] proposed Local Derivative Pattern (LDP) to capture more detailed information by introducing high order derivatives. However, if the order is greater than three, LDP is more sensitive to noise than LBP. Guo *et al*. [15] proposed Completed LBP (CLBP) by combining the original LBP with the measures of local intensity difference and central pixel gray-level.

Although these aforementioned LBPs mentioned above achieve impressive classification accuracy by considering the micro-structure, the micro-structure is not absolutely invariant to rotation under the huge illumination changes as discussed in [16]. Therefore, Zhao *et al*. [16] proposed a novel local pattern, that is, the Local Binary Count (LBC), to address rotation invariant texture classification by totally discarding the micro-structure. Although the local structure information is abandoned, LBC obtains the same performance as LBP in rotation invariant cases. LBC (or LBP) is sensitive to random noise and quantization noise in the near-uniform regions, as the LBC (or LBP) threshold is the value of the central pixel in [13]. Besides, CLBP and CLBC do not consider a comprehensive relationship among all of the pixels in the local region as mentioned in [17]. Zhao *et al*. [18] presented Completed Robust Local Binary Pattern (CRLBP) for texture classification to address noise by modifying the center pixel gray-level to improve the LBP, but the improvement is subtle and a more parameter has to be tuned.

Motivated by the center-symmetric strategy introduced in [11], the high order derivative presented in [14], the limited relationship information among the pixels in the local binary region discussed in [17], and the weighted gray local level trick introduced in [18], this paper tries to address these potential difficulties by proposing a hybrid framework of LBP, called Completed Hybrid Local Binary Pattern (CHLBP). In CHLBP, a second order derivative is introduced and a strategy is presented to combine the first order derivative with the second order derivative. To make the proposed model more robust and stable, the value of each center pixel in a 3×3 local region is replaced by its average local gray level and the value of each neighbor pixels are also modified. Compared to gray value, the average local gray level is more robust to noise, illumination variants and view point variants. Experimental results show that CHLBP achieves higher classification rates than other variants of LBP and is less sensitive to noise, illumination variations and viewpoint variations.

The remainder of this paper is organized as follows. Section II briefly reviews LBP, CS-LBP and CLBP. Section III presents the framework of CHLBP. Section IV reports experimental results and Section V concludes the whole paper.

II. Related Work

As we have pointed out above, the original LBP descriptor has some demerits. For example, LBP is sensitive to illumination variations, and sometimes it tends to describe different local patterns with the same binary code, which will reduce its discriminability inevitably. In the past years, to improve the original LBP, several new improved version of LBP have been proposed. In this section, we will briefly introduce two demerits of LBP and its two improved versions, i.e., the Center-Symmetric LBP (CS-LBP) [11] and the Completed Local Binary Pattern (CLBP) [15].

A. Brief Review of Local Binary Pattern (LBP)

In order to address gray-scale and rotation invariant texture classification, Ojala *et al*. [10] proposed a theoretically very simple, yet efficient, multiresolution approach based on local binary pattern. As shown in Fig. 1. Derived from a circularly symmetric neighbor set of pixels in a local neighborhood, the Local Binary Pattern (LBP) is invariant against any monotonic transformation of the gray scale and can be described by the following formula:

$$\mathrm{LBP}_{P,R} = \sum_{p=0}^{P-1} s\left(g_p - g_c\right) 2^p, \quad s(x) = \begin{cases} 1, x \geq 0 \\ 0, x < 0 \end{cases} \tag{1}$$

where P is the size of the neighbor set of pixels in a local neighborhood, R is the radius of the local region, g_c represents the gray value of the center pixel and g_p ($p = 0, 1, \dots, P-1$) denotes the gray value of the neighbors. Suppose the coordinate of g_c is $(0, 0)$, then the coordinates of g_p are $(R\cos(2\pi p/P), R\sin(2\pi p/P))$. The gray values of neighbor pixels that are not in the image grids are estimated by bilinear interpolation.

In [10], the rotation invariant LBP, denoted as $\mathrm{LBP}_{P,R}^{\mathrm{ri}}$, in which the superscript $^{\mathrm{ri}}$ refers to the rotation invariant patterns, is defined as:

$$\mathrm{LBP}_{P,R}^{\mathrm{ri}} = \min\left\{ROR\left(\mathrm{LBP}_{P,R}, i\right) \middle| i = 0, 1, \dots, P-1\right\} \tag{2}$$

where P and R are defined as in (1), and $ROR(x, i)$ performs a circular bit-wise shift right on the P-bit number x i times.

Furthermore, Ojala *et al*. [10] observed that certain patterns occupy the vast majority, sometimes over 90 percent among all LBP patterns. Based on this observation, a uniformity measure U, the number of spatial transitions (bitwise 0/1 changes) of LBP pattern is defined as follows $U(x)$:

$$U(x) = \sum_{n=0}^{N-1} \left| b(x, n) - b\left(x, (n+1) \bmod N\right) \right| \tag{3}$$

where N is an positive integer, x is an N-bit binary integer, and $b(x, n)$ gets the value of the n-th bit of x. And $U(\mathrm{LBP}_{P,R})$ can be calculated as follows:

$$U\left(\mathrm{LBP}_{P,R}\right) = \sum_{p=0}^{P-1} \left| s\left(g_p - g_c\right) - s\left(g_{(p+1) \bmod P} - g_c\right) \right|. \tag{4}$$

And the uniform LBP patterns, named $\mathrm{LBP}_{P,R}^{\mathrm{u2}}$, are the patterns which have limited transition in the circular binary presentation [10]. The rotation invariant forms of the uniform patterns are denoted as $\mathrm{LBP}_{P,R}^{\mathrm{riu2}}$, in which the superscript $^{\mathrm{riu2}}$ refers to the rotation invariant uniform patterns. With the same notations used above, $\mathrm{LBP}_{P,R}^{\mathrm{riu2}}$ is defined as follows:

$$\mathrm{LBP}_{P,R}^{\mathrm{riu2}} = \begin{cases} \sum_{p=0}^{P-1} s\left(g_p - g_c\right), & U\left(\mathrm{LBP}_{P,R}\right) \leq 2 \\ P+1, & U\left(\mathrm{LBP}_{P,R}\right) > 2 \end{cases} \tag{5}$$

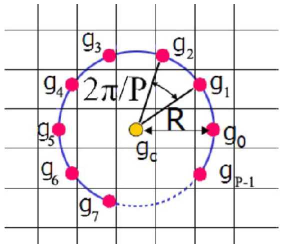

Fig. 1. Central pixel and its P circularly and evenly spaced neighbors with radius R [15]

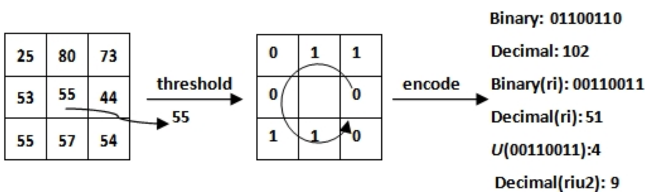

Fig. 2. Illustration of the LBP process.

For a specific value P, $\mathrm{LBP}_{P,R}$, $\mathrm{LBP}_{P,R}^{\mathrm{u2}}$ and $\mathrm{LBP}_{P,R}^{\mathrm{riu2}}$ have 2^P, $P*(P-1)+3$ and $P+2$ distinct coding values, respectively. The mapping from $\mathrm{LBP}_{P,R}$ to $\mathrm{LBP}_{P,R}^{\mathrm{ri}}$, $\mathrm{LBP}_{P,R}^{\mathrm{u2}}$ or $\mathrm{LBP}_{P,R}^{\mathrm{riu2}}$ can be easily implemented with a lookup table. As rotation invariant is very necessary for texture classification, we shall mainly discuss rotation invariant uniform LBP patterns in this paper. After the $\mathrm{LBP}_{P,R}^{\mathrm{riu2}}$ code of each pixel is defined, a histogram will be constructed to represent the texture image.

LBP is simple and efficient. However, a little change of the center pixel may greatly affects LBP code. For example, if the center pixel is shifted from 55 to 58 in Fig. 2, the coding values of $\mathrm{LBP}_{P,R}$, $\mathrm{LBP}_{P,R}^{\mathrm{ri}}$ and $\mathrm{LBP}_{P,R}^{\mathrm{riu2}}$ are changed from 102, 51 and 9 to 96, 3 and 2, respectively. Aiming at this demerit, Tan and Riggs [13] extended original LBP to 3-valued LTP. Although LTP code are more robust to noise, it is no longer strictly invariant to monotonic gray scale transformations.

B. B. *Brief review of Center-Symmetric Local Binary Pattern (CS-LBP)*

In order to describe interest regions, Heikkila *et al.* [11] presented Center-Symmetric LBP (CS-LBP) by comparing center-symmetric pairs of pixels instead of comparing neighbors with the center pixel, which produces more compact binary patterns. $\text{CS-LBP}_{P,R}$ only produces $2^{P/2}$ different binary patterns, whereas for $\mathrm{LBP}_{P,R}$ the number is 2^P. By applying a threshold with a small value T to the gray-level differences, robustness on flat image regions is obtained:

$$\text{CS-LBP}_{P,R,T} = \sum_{p=0}^{P/2-1} s\left(g_p - g_{p+(p/2)}\right)2^p,\; s(x) = \begin{cases} 1, x \ge T \\ 0, x < T \end{cases} \quad (6)$$

where P, R and g_p are defined as in (1).

For several applications, CS-LBP gives better results than LBP [11] due to the dimensionality and the fact that the CS-LBP captures better the gradient information than the basic LBP. However, CS-LBP still suffers from performance reduction, as it ignores the center pixel, whose intensity value can contribute useful information [15].

C. *Brief Review of Completed Local Binary Pattern (CLBP)*

The original LBP also suffers from the demerit that many different structural patterns may have the same LBP code. As illustrated in Fig. 3, pattern (a) and (b) have quite different local structure in spite of the same LBP code.

Aiming to improve the discriminative capability of the local structure, the image local differences (d_p) are decomposed into two complementary components [15], i.e., the signs (s_p) and the magnitudes (m_p), respectively:

$$\begin{aligned} d_p &= s_p * \mathrm{m}_p, \\ s_p &= s\left(g_p - g_c\right), \quad p = 0, 1, \ldots, P \\ m_p &= \left|g_p - g_c\right|, \end{aligned} \quad (7)$$

where P, g_p, g_c and $s(x)$ are defined as in (1). Two operators, CLBP-Sign (CLBP_S) and CLBP-Magnitude (CLBP_M) are proposed to encode them, in which CLBP_S is equivalent to the conventional LBP, and CLBP_M measures variance of magnitude. The CLBP_M can be defined as follows:

$$\mathrm{CLBP\_M}_{P,R} = \sum_{p=0}^{P-1} s\left(m_p - m_I\right)2^p \quad (8)$$

where threshold m_I is set as the average value of m_p of the whole image. Similar to CLBP_S, we can define the rotation invariant uniform patterns for CLBP_M, denoted as $\mathrm{CLBP\_M}_{P,R}^{\mathrm{riu2}}$ as follows:

$$\mathrm{CLBP\_M}_{P,R}^{\mathrm{riu2}} = \begin{cases} \sum_{p=0}^{P-1} s\left(m_p - m_I\right), & U\left(\mathrm{CLBP\_M}_{P,R}\right) \le 2 \\ P+1, & U\left(\mathrm{CLBP\_M}_{P,R}\right) > 2 \end{cases} \quad (9)$$

where m_p and m_I are defined as in (8), and $U(x)$ is defined as in (3).

Based on the observation that the center pixel also capture discriminative information, Guo *et al.* [15] also defined an operator CLBP-Center (CLBP_C) to characterize the central information as follows:

$$\mathrm{CLBP\_C}_{P,R} = s\left(g_c - c_I\right) \quad (10)$$

where P, R, g_c and $s(x)$ are defined as in (1), and threshold c_I is set as the mean gray-level of the whole image. By combining the three operators of CLBP_S, CLBP_M and CLBP_C, denoted as CLBP_S/M/C , notable improvement is made for differentiating the confusing patterns.

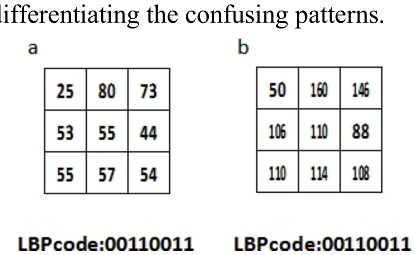

Fig. 3. An example that LBP represent different structural patterns with the same binary code

Although CLBP is superior to LBP as far as the ability to discriminate different structural patterns is concerned, CLBP may also assign the same coding value to structures that seems different to each other [18]. Besides, CLBP is also sensitive to noise as the center pixel gray level is used as the threshold directly.

III. COMPLETED HYBRID LOCAL BINARY PATTERN (CHLBP)

In order to address these aforementioned difficulties, in this section, we propose a hybrid framework of LBP which inherits the merits of CS-LBP and CLBP, but can overcome their flaws.

A. Order-based Center-Symmetric Local Binary Pattern (OCS-LBP)

LBP in nature represent a first order circular derivative pattern of images. However, the first order pattern fails to extract more detailed information in the texture image [14]. In fact, a high order operator can capture more detailed discriminative information. On the other hand, the high order derivative tends to be sensitive to noise.

Aiming to exploit more detailed information, we propose the Order-based Center-Symmetric LBP (OCS-LBP) as a complementary to the original LBP. The $\text{OCS-LBP}_{P,R}$ is defined as follows:

$$\begin{aligned}&\text{OCS-LBP}_{P,R}\\&=\sum_{p=0}^{(P/2)-1} s\left(\left(\left(g_p-g_c\right)-\left(g_{p+(P/2)}-g_c\right)\right)/2\right)2^p\\&=\sum_{p=0}^{(P/2)-1} s\left(\left(g_p+g_{p+(P/2)}\right)/2-g_c\right)2^p\end{aligned} \tag{11}$$

where P, R, g_p, g_c and $s(x)$ are defined as in (1). It is obvious that $((g_p - g_c) - (g_{p+(P/2)} - g_c))$ is a second order derivative at the center pixel. As a high order derivative operator, OCS-LBP can capture more detailed discriminative information, i.e., the convexity-concavity of the gray-level which can characterize the change trend of the gray-level.

We also introduce the rotation invariant uniform patterns for OCS-LBP, denoted as $\text{OCS-LBP}_{P,R}^{\text{riu2}}$ and is defined as follows:

$$\text{OCS-LBP}_{P,R}^{\text{riu2}} = \begin{cases}\sum_{p=0}^{(P/2)-1} s\left(\left(g_p+g_{p+(P/2)}\right)/2-g_c\right), & U\left(\text{OCS-LBP}_{P,R}\right)\le 2\\ (P/2)+1, & U\left(\text{OCS-LBP}_{P,R}\right)>2\end{cases} \tag{12}$$

where $U(x)$ is defined as in (3). For a certain value P, $\text{OCS-LBP}_{P,R}^{\text{riu2}}$ has $(P/2)+2$ distinct coding values. Motivated by CLBP, We also introduce Completed OCS-LBP (OCS-CLBP). Using the same notations in (1), the magnitude m_p is defined as follows:

$$m_p=\left|\left(g_p+g_{p+(P/2)}\right)/2-g_c\right|,\quad p=0,1,\ldots,(P/2). \tag{13}$$

Therefore, the variance of magnitude can be measured by OCS-CLBP-Magnitude (OCS-CLBP_M), which is defined as follows:

$$\text{OCS-CLBP\_M}_{P,R}=\sum_{p=0}^{(P/2)-1} s\left(m_p-m_I\right)2^p \tag{14}$$

where P, R and $s(x)$ are defined as in (1), m_p is defined as in (13), and the threshold m_I is set as the mean value of m_p of the whole image. Using the same notations defined as in (13) and (14), we define the rotation invariant uniform $\text{OCS-CLBP\_M}_{P,R}$ as follows:

$$\text{OCS-CLBP\_M}_{P,R}^{\text{riu2}} = \begin{cases}\sum_{p=0}^{(P/2)-1} s\left(m_p-m_I\right), & U\left(\text{OCS-CLBP\_M}_{P,R}\right)\le 2\\ (P/2)+1, & U\left(\text{OCS-CLBP\_M}_{P,R}\right)>2\end{cases}. \tag{15}$$

In addition, We use the same definition given in (10) for OCS-CLBP_C.

B. Hybrid Local Binary Pattern (HLBP)

As mentioned above, the original LBP can capture first order information, while the proposed OCS-LBP can better describe the second order information, in this section we aim to fully exploit these information and introduce a more discriminative operator to characterize the local patterns. By combining these complementary operators, the original LBP and the proposed OCS-LBP, with the joint strategy introduced in [15], we present a Hybrid Local Binary Pattern (HLBP) operator. In order to achieve rotation invariant and reduce computation complexity, we adopt the rotation invariant uniform patterns to construct the HLBP, which is denoted as $\text{HLBP}_{P,R}^{\text{riu2}}$ and defined as follows:

$$\text{HLBP}_{P,R}^{\text{riu2}}=\text{LBP}_{P,R}^{\text{riu2}}*\left(P/2+2\right)+\text{OCS-LBP}_{P,R}^{\text{riu2}} \tag{16}$$

After simple derivation, we can see that $\text{HLBP}_{P,R}^{\text{riu2}}$ has $(P+2)*((P/2)+2)$ distinct coding values.

As OCS-LBP can capture more detailed discriminative information, HLBP outperforms the original LBP.

C. Completed Hybrid Local Binary Pattern (CHLBP)

As aforementioned, the original LBP suffers the demerit that many different structural patterns may have same LBP code, so it is with HLBP. Motivated by CLBP, we present a hybrid framework of LBP, Completed Hybrid Local Binary Pattern (CHLBP), based on the proposed HLBP above.

In practice, The rotation invariant uniform patterns are used to represent the image for the reason of computation complexity. In this paper we adopt rotation invariant uniform patterns in CHLBP, which is decomposed into three operators, CHLBP-Sign (CHLBP_S), CHLBP-Magnitude (CHLBP_M), CHLBP-Center (CHLBP_C). As the reason mentioned above, CHLBP_S is equivalent to $\text{HLBP}_{P,R}^{\text{riu2}}$ as defined in (16). Adopting the same hybrid strategy used in defining $\text{HLBP}_{P,R}^{\text{riu2}}$, we define CHLBP_M ($\text{CHLBP\_M}_{P,R}^{\text{riu2}}$) as follows:

$$\text{CHLBP\_M}_{P,R}^{\text{riu2}} = \text{CLBP\_M}_{P,R}^{\text{riu2}} * (P/2+2) + \text{OCS-CLBP\_M}_{P,R}^{\text{riu2}} \quad (17)$$

where P and R are defined as in (1), $\text{CLBP\_M}_{P,R}^{\text{riu2}}$ is defined as in (9), and $\text{OCS-CLBP\_M}_{P,R}^{\text{riu2}}$ is defined as in (15). Similar to $\text{HLBP}_{P,R}^{\text{riu2}}$, CHLBP_M ($\text{CHLBP\_M}_{P,R}^{\text{riu2}}$) also has $(P+2)*((P/2)+2)$ distinct coding values. We use the same definition given in (10) for CHLBP_C. To use CHLBP_S, CHLBP_M and CHLBP_C to represent images, we adopt the same combination strategy presented in [15].

As so far, The proposed CHLBP is invariant to monotonic gray-scale transformations and rotation invariant and has more ability to discriminate the different local structures. However it is sensitive to noise as the abrupt selection of the threshold and the direct value assigned to the neighbors in the local region. Inspired by [18], we introduce the Average Local Gray Level (ALG), which is insensitive to noise and invariant to monotonic gray scale transformations, to address this demerit. As we can see, it is simple yet effective strategy. We define ALG_c for the threshold as follows:

$$\text{ALG\_c} = \left(g + \sum_{i=0}^{7} g_i\right) \Big/ 9 \quad (18)$$

where P, and R are defined as in (1), g denotes the gray value of the central pixel in a 3×3 local region, and $g_i (i=0,1,\ldots,7)$ represents the gray value of the neighbor pixel. As ALG_c represent the average gray-level of local texture, it is obvious that ALG_c is more robust to noise than the gray value of the center pixel. Similarly, we define $ALG\_\text{n}(p)$ to modify the value of the neighbors on the circle as follows:

$$ALG\_\text{n}_{P,R}(p) = \left(g_{(p-1)\bmod P} + g_p + g_{(p+1)\bmod P}\right) \Big/ 3, \quad p=0,1,\ldots,P-1 \quad (19)$$

where P, R and g_p are defined as in (1). By applying the ALG strategy to the proposed CHLBP process, we can get more robust local patterns.

Experimental results shown that LBP and its variants achieve impressive performance with the introduced AGL strategy in texture classification. We also observed that the selection of local difference set used in built CLBP_M could make a positive difference on the performance of CLBP. By discarding m_p of which the corresponding d_p is negative, we can expect a better result.

IV. Experimental Results

To evaluate the effectiveness of the proposed method, we carried out a series experiments on two large and comprehensive texture databases: the Outex database (see Fig. 4) [19], which includes 24 classes of textures collected under three illuminations and at nine angles, and the UIUC database (see Fig. 5) [20], which contains 25 classes of real-world textures under significant viewpoint variations.

A. Methods in Comparison and Dissimilarity Measure

As LBP-based schemes, the proposed OCS-CLBP and CHLBP are compared with the representative LBP scheme in [10], the CLBP algorithm in[15], and the CRLBP method in [18].

As mentioned above, in the following discussion, we only consider the rotation invariant uniform patterns and use the combination strategy and notation method introduced in [15]. For the LBP scheme we choose the $\text{LBP}_{P,R}^{\text{riu2}}$ operator, denoted as LBP; for CLBP methods, we use $\text{CLBP\_M}_{P,R}^{\text{riu2}}$ and $\text{CLBP\_S}_{P,R}^{\text{riu2}}/\text{M}_{P,R}^{\text{riu2}}/\text{C}$ operator, denoted as CLBP_M and CLBP_S/M/C, respectively; for the CRLBP algorithm, we utilize the $\text{CRLBP\_S}_{P,R}^{\text{riu2}}/\text{M}_{P,R}^{\text{riu2}}/\text{C}$ operator, denoted as CRLBP. All these selected operators can achieve impressive results. And for the proposed OCS-CLBP method, we use operator $\text{OCS-CLBP\_S}_{P,R}^{\text{riu2}}/\text{M}_{P,R}^{\text{riu2}}/\text{C}$, denoted as OCS-CLBP; for the proposed CHLBP model, we use operator $\text{HLBP\_S}_{P,R}^{\text{riu2}}$, $\text{CHLBP\_M}_{P,R}^{\text{riu2}}$, $\text{CHLBP\_M}_{P,R}^{\text{riu2}}/\text{C}$, $\text{CHLBP\_M}_{P,R}^{\text{riu2}}\_\text{S}_{P,R}^{\text{riu2}}/\text{C}$, denoted as CHLBP_S, CHLBP_M, CHLBP_M/C, CHLBP_M_S/C, respectively. We use alg_i to denote what ALG strategy, defined as in (18) and (19), is applied to the methods: no ALG strategy is applied when $i=0$; the strategy ALG_c is adopted when $i=1$; the strategy $ALG\_\text{n}(p)$ is adopted when $i=2$; and ALG_c and $ALG\_\text{n}(p)$ are all applied at the same time when $i=3$.

In the past years, several measures have been proposed for discriminating the dissimilarity between two histograms [25], [28], [29]. In this paper, we adopt the χ^2 statistics to

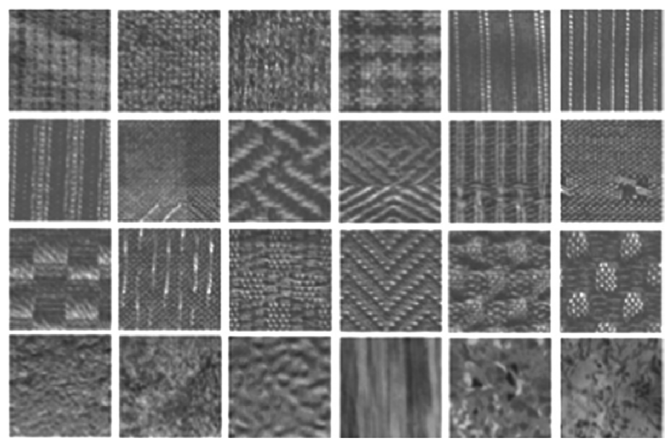

Fig. 4. 24 texture images from the Outex database.

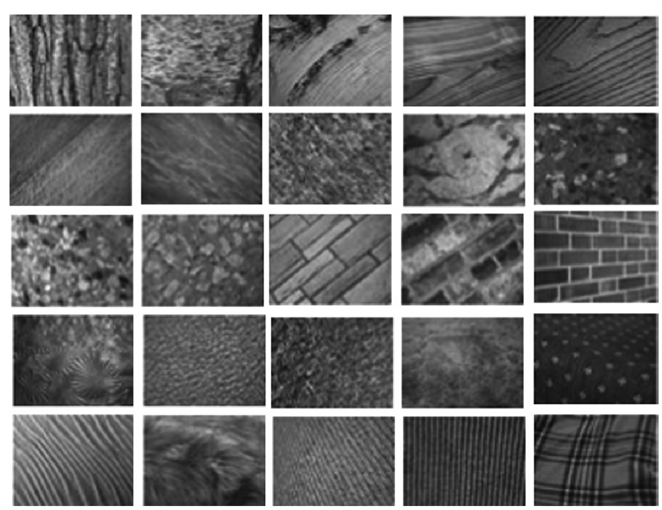

Fig. 5. 25 texture images from the UIUC database.

TABLE I.
CLASSIFICATION RATE (%) ON OUTEX (TC10 AND TC12) USING DIFFERENT METHODS

	$R=1, P=8$				$R=2, P=16$				$R=3, P=24$			
	TC10	TC12		Average	TC10	TC12		Average	TC10	TC12		Average
		t184	horizon			t184	horizon			t184	horizon	
LBP	84.82	65.46	63.68	71.32	89.40	82.27	75.21	82.29	95.08	85.05	80.79	86.97
CLBP_M	81.74	59.31	62.78	67.94	93.67	73.80	72.41	79.96	95.52	81.18	78.66	85.12
CLBP_S/M/C	96.56	90.30	92.29	93.05	98.72	93.54	93.91	95.39	98.93	95.32	94.54	96.26
CRLBP (α=1) [18]	96.54	91.16	92.06	93.25	98.85	**96.67**	96.97	**97.50**	99.48	97.57	97.34	98.13
CRLBP (α=8) [18]	**97.55**	**91.94**	**92.45**	**93.98**	98.59	95.88	96.41	96.96	99.35	96.83	96.16	97.45
CLBP_S/M/C (agl_2)	97.27	88.89	91.20	92.45	98.83	94.70	94.72	96.08	99.06	96.13	95.65	96.95
CLBP_S/M/C (agl_3)	96.82	86.27	87.73	90.27	**98.88**	94.86	95.49	96.41	99.30	96.60	95.88	97.26
OCS-CLBP(agl_0)	82.71	72.04	76.27	77.01	95.60	88.06	91.06	91.59	98.20	94.38	95.16	95.91
OCS-CLBP(agl_1)	74.40	69.44	71.79	71.94	96.02	89.21	91.92	92.38	99.01	95.79	97.04	97.28
OCS-CLBP(agl_2)	86.80	73.84	77.57	79.40	95.83	87.11	88.84	90.59	97.73	92.82	93.68	94.79
OCS-CLBP(agl_3)	75.13	67.85	70.00	70.99	94.97	89.07	92.27	92.10	98.88	95.46	97.75	97.36
CHLBP_S (agl_0)	83.33	74.12	76.53	77.99	96.02	90.32	89.21	91.85	98.39	91.74	89.58	93.24
CHLBP_M (agl_0)	84.92	69.26	74.38	76.19	96.02	89.49	90.35	91.95	99.19	95.97	95.21	96.79
CHLBP_M/C (agl_0)	92.68	83.47	85.81	87.32	98.52	92.92	94.05	95.16	99.17	96.48	96.06	97.24
CHLBP_M_S/C(agl_0)	94.11	86.76	90.37	90.41	98.39	94.77	95.56	96.24	99.51	97.59	97.25	98.12
CHLBP_S (agl_1)	78.41	69.44	70.90	72.92	96.54	93.87	92.01	94.14	99.11	93.84	91.50	94.82
CHLBP_M (agl_1)	82.16	72.55	73.56	76.09	96.74	92.38	93.47	94.20	99.04	96.67	96.04	97.25
CHLBP_M/C (agl_1)	86.07	80.76	83.19	83.34	98.62	93.91	94.88	95.80	99.32	96.99	97.45	97.92
CHLBP_M_S/C(agl_1)	87.29	78.61	81.81	82.57	98.85	95.76	**97.04**	97.22	**99.64**	97.94	97.96	98.51
CHLBP_S (agl_2)	86.12	74.17	70.83	77.04	94.40	88.17	86.85	89.81	98.46	92.06	89.70	93.41
CHLBP_M (agl_2)	84.01	65.00	61.60	70.20	96.25	89.61	89.14	91.67	99.04	95.49	95.65	96.73
CHLBP_M/C (agl_2)	93.52	79.63	77.55	83.57	97.55	91.94	93.29	94.26	99.14	96.04	96.23	97.14
CHLBP_M_S/C(agl_2)	93.75	85.14	83.47	87.45	96.77	93.73	94.44	94.98	99.53	97.94	97.41	98.29
CHLBP_S (agl_3)	66.59	63.47	63.63	64.56	95.70	92.15	91.09	92.98	98.75	93.89	92.04	94.89
CHLBP_M (agl_3)	78.91	68.31	71.71	72.98	95.81	91.39	92.71	93.30	99.17	96.57	96.11	97.28
CHLBP_M/C (agl_3)	84.43	77.69	82.38	81.50	96.95	92.92	94.81	94.89	99.30	97.20	**98.33**	98.28
CHLBP_M_S/C(agl_3)	78.93	75.21	78.52	77.55	98.18	96.20	96.57	96.98	99.58	**98.59**	98.17	**98.78**

address this problem. For two histograms, $H=\{h_i\}$ and $K=\{k_i\}$ $(i=1,2,\dots,\mathrm{N})$, the χ^2 statistics can be calculated as follows:

$$d_{\chi^2}(H,K)=\sum_{i=1}^{N}\frac{(h_i-k_i)^2}{h_i+k_i} \tag{20}$$

In addition, in this paper, we assume that the nearest neighborhood classifier is used in all the methods [23][24].

B. Experimental Results on the Outex Database

The Outex database includes two test suites, that is, Outex_TC_00010 (TC10) and Outex_TC_00012 (TC12). The two test suites contain the same 24 classes of textures, which were collected under three different illuminants ("horizon," "inca," and "t184") and nine different rotation angles $(0^\circ, 5^\circ, 10^\circ, 15^\circ, 30^\circ, 45^\circ, 60^\circ, 75^\circ, 90^\circ)$. There are 20 non-overlapping texture samples for each class under a given illumination and rotation angle condition. For TC10, the classifier was trained with samples of illumination "inca" and angle 0° in each class and the testing dataset was constructed by the other eight rotation angles with the same illuminant. Therefore, there are 480 $(24*20)$ and 3840 $(24*20*8)$ images used for models and validation samples, respectively. For TC12, same dataset as TC10 were used for classifier training and all samples captured under illumination "t184" or "horizon" were used as testing samples. Hence, there are 480 $(24*20)$ models and 4320 $(24*20*9)$ validation samples.

Table I lists the experimental results by different schemes, from which we could make the following findings. Firstly, in the experiment $(\mathrm{R}=3,\mathrm{P}=24)$, OCS-CLBP achieve significant performance compared to other methods when the size of the histogram is concerned. It should be noticed that OCS-CLBP also achieves impressive results under illumination "t184" and "horizon". It is obvious that OCS-CLBP does capture more detailed discriminative information. As a result, CHLBP performs better than other algorithm which is validated by the experiment $(\mathrm{R}=3,\mathrm{P}=24)$ on the Outex database. Secondly, whatever AGL strategy is adopted, CHLBP (CHLBP_M_S/C) almost always achieve better results than other methods in the experiment $(\mathrm{R}=3,\mathrm{P}=24)$ on TC12 dataset, which demonstrates CHLBP is more robust to illumination variations. Thirdly, the introduced AGL strategy can improve performance of LBPs, such as, CLBP_S/M/C. Finally, CHLBP_M/C performs better than other methods when the feature dimensionality is concerned. In a word, CHLBP can get higher classification rates than other methods and it is less sensitive to illumination variations.

C. Experimental Results on the UIUC Database

The UIUC texture database contains 1000 texture images with 25 different classes and 40 samples for each class. The resolution of each image is 640×480. The database contains materials imaged under significant viewpoint variations. To get statistically significant experimental results, N training images were randomly chosen from each class while the remaining $40-N$ images per class were used as the validation set. The partition is implemented 100 times independently. The average classification accuracy over 100 randomly splits is listed in Table II.

Similar conclusions to those in Section IV-B can be drawn from the experimental results on the UIUC database. Firstly, the proposed OCS-CLBP achieves impressive results in the experiment $(\mathrm{R}=3,\mathrm{P}=24)$ when the feature

TABLE II.
CLASSIFICATION RATE (%) ON UIUC USING DIFFERENT METHODS

	$R=1, P=8$				$R=2, P=16$				$R=3, P=24$			
	20	15	10	5	20	15	10	5	20	15	10	5
LBP	55.36	51.71	47.66	40.22	60.88	56.83	51.67	42.03	64.21	60.36	54.64	44.82
CLBP_M	57.70	54.94	49.85	42.15	72.27	69.64	65.14	56.24	74.26	70.93	65.74	55.93
CLBP_S/M/C	87.62	85.79	82.61	74.65	91.01	89.32	86.15	78.44	91.05	89.16	85.87	77.69
CRLBP (α=1) [18]	86.91	85.67	82.20	73.95	**92.92**	**91.82**	88.15	**81.98**	93.31	92.03	89.47	**81.90**
CRLBP (α=1) [18]	**88.01**	**86.62**	**82.97**	**76.01**	91.99	90.41	88.04	81.49	92.83	90.55	88.02	80.54
CLBP_S/M/C (agl_2)	84.59	82.61	79.04	70.96	91.22	89.68	86.82	79.79	92.55	90.91	87.85	80.32
CLBP_S/M/C (agl_3)	81.55	79.37	75.47	67.74	92.26	90.86	87.96	80.59	93.28	91.86	88.79	81.07
OCS-CLBP(agl_0)	75.79	73.13	69.21	61.30	85.74	83.73	80.19	72.81	88.66	87.01	83.61	75.98
OCS-CLBP(agl_1)	67.18	64.01	59.36	51.22	88.02	86.38	82.82	75.28	89.95	88.20	84.67	76.99
OCS-CLBP(agl_2)	71.43	69.09	65.21	57.72	83.84	81.92	78.42	71.26	88.90	87.24	83.88	76.63
OCS-CLBP(agl_3)	70.50	67.12	62.38	53.59	88.06	86.71	83.63	77.05	91.09	89.86	86.72	79.96
CHLBP_S (agl_0)	73.65	69.81	64.81	54.98	81.52	77.73	72.34	60.87	86.12	8285	77.33	65.72
CHLBP_M (agl_0)	72.27	69.16	65.21	56.27	85.41	82.45	78.31	68.51	89.43	86.40	81.89	71.85
CHLBP_M/C (agl_0)	82.00	79.96	76.41	68.40	89.75	87.56	84.00	75.55	91.68	89.32	85.64	76.64
CHLBP_M_S/C (agl_0)	85.26	82.63	78.73	69.77	90.53	88.20	84.62	75.42	92.58	90.37	86.37	77.00
CHLBP_S (agl_1)	65.53	61.75	56.60	47.48	83.35	80.06	74.84	63.96	86.75	84.03	78.91	67.49
CHLBP_M (agl_1)	72.16	69.23	64.73	56.10	87.20	84.39	80.48	70.96	89.82	87.26	83.00	73.00
CHLBP_M/C (agl_1)	81.54	79.54	75.85	68.00	90.82	89.03	85.84	77.80	92.19	90.22	86.78	77.73
CHLBP_M_S/C (agl_1)	72.77	69.41	63.38	52.24	92.05	90.12	86.53	77.57	93.29	91.26	87.59	78.23
CHLBP_S (agl_2)	63.86	59.80	54.93	43.60	80.51	77.12	71.55	60.34	87.71	84.59	79.52	67.59
CHLBP_M (agl_2)	69.08	65.77	60.80	51.81	85.09	82.39	78.35	68.40	89.86	87.19	83.13	73.10
CHLBP_M/C (agl_2)	76.52	73.87	69.13	60.59	88.20	85.96	82.36	74.28	91.21	89.08	85.49	77.00
CHLBP_M_S/C (agl_2)	81.91	78.87	74.39	64.95	89.98	87.85	84.47	75.79	93.11	91.03	87.40	78.59
CHLBP_S (agl_3)	61.33	57.44	52.49	43.30	84.44	81.30	76.72	66.34	89.19	86.35	81.65	70.47
CHLBP_M (agl_3)	73.89	70.71	65.95	57.05	87.98	85.60	81.94	73.05	91.02	88.84	85.01	75.45
CHLBP_M/C (agl_3)	80.42	78.25	74.51	66.77	91.20	89.72	86.61	79.56	92.68	91.11	88.10	80.01
CHLBP_M_S/C (agl_3)	76.50	72.97	67.43	56.28	92.67	91.05	**88.24**	80.53	**94.56**	**92.96**	**89.80**	81.25

dimensionality and computation complexity are concerned, as OCS-CLBP (agl_3) produce much better results than CLBP especially when the size of the training set is small. Secondly, CHLBP (CHLBP_M_S/C(agl_3)) performs much better than CLBP when the radius is larger than one. Thirdly, CHLBP also achieves much better accuracy results than CRLBP in the experiment ($\mathrm{R}=3, \mathrm{P}=24$). In addition, The proposed ALG_n(p) strategy can make CLBP and its variants more effective. In one word, CHLBP achieves higher classification accuracy and less sensitive to viewpoint variations and illumination variations than other LBP-based methods.

V. CONCLUSIONS

In this paper, we analyzed the two main demerits of Local Binary Pattern (LBP). And then we proposed a novel Order-based Center-Symmetric Local Binary Pattern (OCS-LBP) which could capture more detailed discriminative information. Based on LBP and the proposed OCS-LBP, we presented a new hybrid framework of LBP, named Completed Hybrid Local Binary Pattern. We also introduced a simple yet effective strategy, the Average Local Gray Level (ALG), which could make the CHLBP model less sensitive to illumination variations and viewpoint variations. Experimental results obtained from two representative databases clearly demonstrate that the proposed CHLBP method enhanced by AGL strategy is less sensitive to illumination variations and viewpoint variations and can obtain impressive texture classification accuracy.

ACKNOWLEDGMENT

The authors would like to sincerely thank the Center for Machine Vision Research and Z. Guo for sharing the source codes of Local Binary Pattern and Completed Local Binary Pattern. This work was supported by the grants of the National Science Foundation of China, Nos. 61373098 & 61373105, and the Outstanding Innovative Talent Program Foundation of Henan Province, No. 134200510025.

REFERENCES

[1] J.-G. Zhang, and T.-N. Tan, "Brief review of invariant texture analysis methods," Pattern Recognition, vol. 35, no. 3, pp. 735-747, Mar. 2002.

[2] L.S. Davis, "Polarograms—a new tool for image texture analysis," Pattern Recognition , vol. 13, no. 3, pp. 219–223,1981.

[3] J. Duvernoy, "Optical digital processing of directional terrain textures invariant under translation, rotation, and change of scale," Appl. Opt. vol. 23, no. 6, pp. 828–837, 1984.

[4] R.K. Goyal, W.L. Goh, and D.P. Mitaletal, "Scale and rotation invariant texture analysis based on structural property," in Conf. Jan. 1995 IEEE Int. Conf. Industrial Electronics, Control, and Instrumentation, pp.1290–1294, 1995.

[5] G. Eichmann, and T. Kasparis, "Topologically invariant texture descriptors," Comput. Vision Graphics Image Process. , vol. 41, no. 3, pp. 267–281, 1988.

[6] R.L. Kashyap, and A. Khotanzad, "A model-based method for rotation invariant texture classification," IEEE Trans. Pattern Anal. Mach. Intell., vol. 8, no. 4, pp. 472–481, 1986.

[7] F.S. Cohen, Z.G. Fan, and M.A. Patel, "Classification of rotated and scaled textured images using Gaussian Markov random field models," IEEE Trans. Pattern Anal. Mach. Intell. vol. 13, no. 2, pp. 192–202, 1991.

[8] J.L. Chen, and A. Kundu, "Rotation and gray scale transform invariant texture recognition using hidden Markov model,", in Conf. Jan. 1992 Int. Conf. on Acoustics, Speech, and Signal Processing, Icassp, 1992, pp. C69–C72.

[9] R. Porter, and N. Canagarajah, "Robust rotation invariant texture classification," in Conf. 1997 IEEE Int. Conf. on Acoustics, Speech, and Signal Processing, I–V,1997,pp.3157–3160.

[10] T. Ojala, M. Pietikainen, and T. Maenpaa, “Multiresolution gray-scale and rotation invariant texture classification with local binary patterns,” IEEE Trans. Pattern Anal. Mach. Intell. vol. 24, no. 7, pp. 971–987, 2002.

[11] M. Heikkila, M. Pietikainen, and C. Schmid, “Description of interest regions with center-symmetric local binary patterns,” in Proc. of Computer Vision, Graphics and Image Processing 4338, pp. 58–69. 2006.

[12] S. Liao, M.W. K. Law, and A.C.S. Chung, “Dominant local binary patterns for texture classification,” IEEE Trans. Image Process., vol. 18, no. 5, pp. 1107–1118, 2009.

[13] X.Y. Tan, and B. Triggs, “Enhanced local texture feature sets for face recognition under difficult lighting conditions,” IEEE Trans. Image Process., vol. 19, no. 6, pp. 1635–1650, 2010.

[14] B. Zhang, Y. Gao, S. Zhao, and J. Liu, “Local derivative pattern versus local binary pattern: Face recognition with high-order local pattern descriptor,” IEEE Trans. Image Process., vol. 19, no. 2, pp. 533-544, 2010.

[15] Z.H. Guo, L. Zhang, and D. Zhang, “A completed modeling of local binary pattern operator for texture classification,” IEEE Trans. Image Process. vol. 19, no. 6, pp. 1657–1663, 2010.

[16] Y. Zhao, D.-S Huang, and W. Jia, “Completed Local Binary Count for Rotation Invariant Texture,” IEEE Trans. on Image Process., vol. 21, no. 10, pp. 4492-4497, 2012.

[17] V.D. Nguyen, D.D. Nguyen, T.T. Nguyen, V.Q. Dinh, and J.W. Jeon, “Support local pattern and its application to disparity improvement and texture classification,” IEEE Trans. Circuits and Systems for Video Technology. vol. PP, no. 99, 2013.

[18] Y. Zhao, W. Jia, R.-X. Hu, and H. Min, “Completed robust local binary pattern for texture classification,” Neurocomputing, vol. 106, pp. 68-76, 2013.

[19] T. Ojala, T. Maenpaa, M. Pietikainen, J. Viertola, J. Kyllönen, and S. Huovinen, “Outex - new framework for empirical evaluation of texture analysis algorithms,” in Proc. 16th Int. Conf. Pattern Recognit., vol. 1, pp. 701–706, 2002.

[20] S. Lazebnik, C. Schmid, and J. Ponce, “A sparse texture representation using local affine regions,” IEEE Trans. Pattern Anal. Mach. Intell., vol. 27, no. 8, pp. 1265–1278, Aug. 2005.

[21] X. F. Wang, D.S. Huang, and H. Xu, “An efficient local Chan-Vese model for image segmentation,” Pattern Recognition, vol. 43, no.3, pp. 603-618, 2010.

[22] B. Li, and D.S. Huang, “Locally linear discriminant embedding: An efficient method for face recognition,” Pattern Recognition, vol.41, no.12, pp. 3813-3821, 2008.

[23] D.S. Huang, and J.-X. Du, “A constructive hybrid structure optimization methodology for radial basis probabilistic neural networks,” IEEE Trans. Neural Networks, vol. 19, no.12, pp 2099-2115, 2008.

[24] D.S. Huang, “Radial basis probabilistic neural networks: Model and application,” Int. Journal of Pattern Recognit., and Artificial Intell,, vol. 13, no. 7, pp.1083-1101, 1999.

[25] X.-F. Wang, and D.S. Huang, “A novel density-based clustering framework by using level set method,” IEEE Trans. Knowledge and Data Engineering, vol. 21, no.11, pp 1515-1531, 2009.

[26] L. Shang, D.S. Huang, J.-X. Du, and C.-H. Zheng, “ Palmprint recognition using Fast ICA algorithm and radial basis probabilistic neural network,” Neurocomputing, vol.69, no. 13-15, pp. 1782-1786, 2006.

[27] Z.-Q. Zhao, D.S. Huang, and B.-Y. Sun, “Human face recognition based on multiple features using neural networks committee,” Pattern Recognition Letters, vol.25, no.12, pp.1351-1358, 2004.

[28] D.S. Huang, Horace H.S.Ip and Z.-R. Chi, “A neural root finder of polynomials based on root moments,” Neural Computation, vol.16, no.8, pp.1721-1762, 2004.

[29] D.S. Huang, “A constructive approach for finding arbitrary roots of polynomials by neural networks,” IEEE Trans. on Neural Networks, vol.15, no.2, pp.477-491, 2004.